NATIONAL ADVISORY COMMITTEE FOR AERONAUTICS

TECHNICAL NOTE 3955

A COLLECTION OF DATA FOR ZERO-LIFT DAMPING IN ROLL OF WING-BODY COMBINATIONS AS DETERMINED WITH ROCKET-POWERED MODELS EQUIPPED WITH ROLL-TORQUE NOZZLES

By David G. Stone

Langley Aeronautical Laboratory
Langley Field, Va.

Washington
April 1957

NATIONAL ADVISORY COMMITTEE FOR AERONAUTICS

TECHNICAL NOTE 3955

A COLLECTION OF DATA FOR ZERO-LIFT DAMPING IN ROLL OF WING-BODY COMBINATIONS AS DETERMINED WITH ROCKET-POWERED MODELS EQUIPPED WITH ROLL-TORQUE NOZZLES[1]

By David G. Stone

SUMMARY

The zero-lift damping-in-roll derivative has been experimentally determined through high subsonic, transonic, and low supersonic speeds by a torque-nozzle forced-roll technique utilizing rocket-propelled models. The data have been collected from investigations using this technique for three-semispan-wing configurations to show the effects of wing plan form and airfoil section and, qualitatively, the effects of aeroelasticity.

This collection of data indicates that the zero-lift damping in roll for wings of aspect ratio less than 6 of a wide variety of plan forms is well defined from subsonic to low supersonic speeds and shows all wings tested to have damping in roll in this speed range at 0° angle of attack. The trends of the effects of the various geometric parameters are about as predicted by theory, even though the level of damping is consistently lower than that obtained by theory.

INTRODUCTION

The damping-in-roll derivative is an important factor in the dynamic lateral behavior of aircraft. In view of this fact, a great amount of testing with various techniques has been done on general and specific configurations. One test technique employed by the Langley Pilotless Aircraft Research Division to obtain the damping in roll at zero lift was the so-called torque-nozzle technique utilizing rocket-propelled models (ref. 1). In this method a known nonaerodynamic forcing moment from the rocket torque nozzle produces roll, and, by measurements of the inertia of the model, Mach number, and rolling velocity, the damping in roll can

[1]Supersedes recently declassified NACA Reseach Memorandum L53E26 by David G. Stone, 1953.

be determined with reasonable accuracy. A more or less systematic series of wings were tested at transonic and low supersonic speeds with each phase or group being reported by the National Advisory Committee for Aeronautics in seven separate papers (refs. 1 to 7). The purpose of this report is to collect the data in one paper from the investigations of this completed program so that the effects of wing geometry and Mach number may be summarized.

SYMBOLS

C_l	rolling-moment coefficient, M_X/qS_nb
C_{l_p}	damping-in-roll derivative, $\Delta C_l/\Delta \frac{pb}{2V}$
M_X	rolling moment, ft-lb
p	rolling angular velocity, radians/sec
q	dynamic pressure, lb/sq ft
M	Mach number
V	velocity, ft/sec
A	aspect ratio, b^2/S_n when $n = 2$
Λ	angle of sweep of wing quarter-chord line, deg
Λ_{LE}	angle of sweep of wing leading edge, deg
Λ_{TE}	angle of sweep of wing trailing edge, deg
λ	taper ratio (ratio of tip chord to chord at body center line)
t/c	airfoil-section thickness ratio parallel to center line
b	wing span (diameter of circle generated by wing tips), ft
D	maximum diameter of body, ft
S_n	area of n semispan wings with wing assumed to extend to model center line, sq ft

n	number of semispan wings
θ/m	wing torsional-stiffness parameter, measured at exposed midspan parallel to model center line, radians/ft-lb
θ	angle of twist, produced by m, at exposed midspan parallel to model center line and normal to wing-chord plane, radians
m	concentrated couple, applied at exposed midspan parallel to model center line and normal to wing-chord plane, ft-lb
$(\theta/m)_{sd}$	calculated θ/m of test wing if fabricated of solid duralumin, radians/ft-lb

MODELS AND TEST TECHNIQUE

The models were simply constructed with minimum internal instrumentation to allow systematic flight testing of various wing configurations. Typical model lines and the locations of unswept, swept, and delta wings on the basic body are shown in figure 1. A complete model consisted of a wooden fuselage with test wings, a nose containing batteries and spinsonde, a ballast tube that attaches to the rocket-motor head cap, and a rocket motor with canted nozzles. The basic principle of this technique is that the model is forced to roll by a nonaerodynamic rolling moment of known magnitude which is produced by the canted nozzle assembly, and the damping in roll is computed by balancing the moments acting on the model. Each model was launched from a rail-type launcher at an elevation angle near 70° to the horizontal and was accelerated to a high subsonic Mach number by means of a booster rocket motor. Then at booster burnout the model was accelerated by the internal rocket motor with canted nozzles to a supersonic Mach number. The Reynolds number range (based on the mean aerodynamic chord) covered for the unswept and swept wings was 2.2×10^6 to 11×10^6 and for the delta wings was 4×10^6 to 17×10^6. A complete description and analysis of this method for determining the damping-in-roll derivative may be found in reference 1. In general, the maximum possible error of the damping-in-roll derivative was ± 0.03 and Mach number measurement was ± 0.01.

The wings used for these tests were of three types, as shown in figure 2, and were constructed of wood with a full-chord duralumin plate in the wing-chord plane, of wood with a duralumin plate plus steel inlays on the section surfaces, and of solid duralumin. The configurations and types of construction used on all the wings are listed in table I. A measure of the torsional stiffness is also listed in table I. The torsional-stiffness parameter θ/m of most of the unswept and swept

wings was obtained by applying a known couple at the exposed midspan and measuring the resulting twist at the midspan. The couple was applied and the twist was measured in planes parallel to the free stream and normal to the wing-chord plane. No stiffness characteristics were measured for the delta wings. In order to establish a relative meaning to the values of torsional-stiffness parameter, the ratios of θ/m of a comparable solid duralumin wing to θ/m of the test wing are given as $\frac{(\theta/m)_{sd}}{\theta/m}$. This can be thought of as a "figure of merit" since few full-scale aircraft wings will be appreciably stiffer than solid duralumin. The values of $(\theta/m)_{sd}$ were calculated for the wings of composite construction. A comparison of the calculated $(\theta/m)_{sd}$ to the measured value for any of the solid duralumin wings indicated that the value of $(\theta/m)_{sd}$ could be determined within 15 percent of the measured value with the largest difference for swept wings; consequently, the values of $\frac{(\theta/m)_{sd}}{\theta/m}$ are given to the nearest tenth only.

Another factor which has influence on the stiffness characteristics is the altitude conditions of the tests. As reported in reference 8, the change in flexibility with altitude varies directly with the ratio of static pressure at test altitude to the sea-level static pressure. This additional flexibility factor, or ratio of static pressures, for all the torque-nozzle-technique models varied from 0.85 ± 0.05 at $M = 1.4$ to 0.65 ± 0.05 at $M = 0.8$.

RESULTS AND DISCUSSION

The damping-in-roll data from the torque-nozzle technique have been collected from references 1 to 7 to show the effects of wing plan form, airfoil section, and number of semispan wings, and, qualitatively, the effect of aeroelasticity. Given in table I is a listing of the various wings for which the derivative C_{l_p} is summarized in this report with samplings of C_{l_p} at $M = 0.8$, $M = 1.0$, and $M = 1.2$, with the figure numbers in which data for each appear, and with the reference number in which the original data were published. Only the damping-in-roll derivative is considered in this report. Wing-dropping phenomenon, as reported in references 9 and 10, in general determines the lateral behavior at transonic speeds without regard for the damping in roll. However, wings that are not susceptible to wing dropping show a smooth retention of damping through the transonic speed region. The methods used to summarize the data are plots of the basic data of C_{l_p} against Mach number for each

geometric parameter with all other parameters, including stiffness, held in a small range of values to eliminate secondary effects as far as possible. The data are for three-semispan-wing configurations, except where the effects of four semispan wings are shown.

Sweepback

The effect of sweepback of the quarter-chord line of untapered wings, moderately tapered wings, and highly tapered wings is shown in figure 3 as collected from references 1, 5, and 6. For these wings, of aspect ratios of 3.5 to 4.0 and 5- and 6-percent thicknesses, sweepback caused an appreciable reduction in C_{l_p}, especially at supersonic speeds and for wings swept more than 45°. As will be shown later, some of this reduction in C_{l_p} at $\Lambda = 60°$ may be an effect of aeroelasticity even though a wing may be made of solid duralumin.

Aspect Ratio

The effect of aspect ratio on unswept untapered wings of 6- and 9-percent thicknesses and swept tapered wings of 9- and 10-percent thicknesses is shown in figure 4 as collected from references 1, 2, 3, and 5. For the 9-percent-thick unswept wings, decrease in the aspect ratio from 4.5 to 2.5 successively decreased C_{l_p} nearly uniformly above $M = 0.95$; whereas, for thinner unswept wings, little difference in C_{l_p} was noted for a decrease of aspect ratio from 4.5 to 3.7. For the swept wings shown in figure 4(c) the effect of increasing the aspect ratio from 3.5 to 6.0 which should increase the damping in roll was not present because of a large aeroelastic effect. This aeroelastic effect can be seen by noting the torsional weakness for these types of construction as compared with that for solid duralumin as shown in table I, and also the aspect-ratio-6 swept wing is approximately 19 times weaker torsionally than the aspect-ratio-3.5 swept wing.

Taper Ratio

The effect of taper ratio on damping in roll for unswept and 45° sweptback wings is shown in figure 5 as obtained from reference 6. For these wings of aspect ratio 3.7 and 6-percent thickness, increasing the taper did not significantly reduce C_{l_p} until the wing was tapered to a point ($\lambda = 0$) at both 0° and 45° sweep. For this set of data, the wings were all as stiff in torsion as solid duralumin, as shown in table I; therefore, probably no aeroelasticity effects exist between the tests of different taper ratios.

Thickness Ratio

The effect of airfoil-section thickness ratio for NACA 6-series airfoil sections on damping in roll for untapered unswept wings and 35° sweptback tapered wings is shown in figure 6, as collected from references 1, 2, 3, and 5. These data, in general, show a small reduction in C_{l_p} at supersonic speeds with increase in thickness ratio with the exception of the unswept wings in figure 6(b) which have a slight change in section shape. The effect of nonuniform thickness ratio for a 35° sweptback wing (fig. 6(c)) was to decrease C_{l_p} slightly which is consistent with the increased-thickness-ratio effect. Also to be noted is how the increasing thickness of the unswept wings increased irregularities in C_{l_p} at transonic speeds which reflects the wing-dropping characteristics as reported in reference 9. The unswept wings for which the data are shown in figure 6 varied appreciably as compared on a torsional-stiffness basis so that aeroelastic effects probably exist in the results.

Airfoil-Section Shape

The effect of airfoil-section shape on damping in roll for unswept and swept wings is shown in figure 7 as obtained from references 2 and 5. A sharp-leading-edge airfoil section can have a significant effect on C_{l_p} of a thin unswept wing as shown in figure 7(a). The double-wedge section had the transonic irregularity in C_{l_p} and produced greater damping in roll at supersonic speeds than the round-nose section. Modifying a 40° sweptback circular-arc-section wing to have undeflected half-slab ailerons with blunt trailing edges over the outer semispan increased the C_{l_p} a small amount and also partially alleviated the irregular transonic behavior (fig. 7(b)). The effects of aeroelasticity are negligible within these comparisons of results on the effect of airfoil-section shape.

Delta Wings

Figure 8 shows the effect of increasing the sweepback of wings of delta plan form and 6-percent thickness (ref. 7) and of increasing the sweepback of a wing of near-delta plan form, or a pointed swept wing (ref. 6). In general, the delta wings had smaller values of C_{l_p} than the other wings of similar aspect ratio and sweep; this is probably the result of the tapering to a point. Moreover, C_{l_p} was reduced uniformly by successive increases in the sweepback of the leading edge or the

accompanying reduction in aspect ratio. As shown in figure 8(a), a 70° sweptback delta wing had about one-half the C_{l_p} of a 45° sweptback delta wing. For a delta wing swept back 60°, the airfoil-section shape had little effect on C_{l_p} as shown in the comparison of the wing with the round-nose hexagonal sections with contour breaks rounded and the NACA 65A006 sections. Because of the length of chord and method of construction (inlays plus plate), the delta wings were probably the most stiff wings tested; therefore, the aeroelastic effects are a minimum in these results.

Increase in Number of Semispan Wings From Three to Four

The effect of increasing the number of semispan wings from three to four is shown in figure 9 for unswept wings and delta wings with leading-edge sweeps of 45°, 60°, and 70°, as collected from references 1, 4, and 7. For the unswept wing an increase in the number of semispan wings to four decreased C_{l_p} and increased the irregularities in C_{l_p}. For the delta wing an increase to four semispan wings had little effect on C_{l_p} until the leading-edge sweep was 70° in which case the small reduction in C_{l_p} was important because of the initial low value of C_{l_p}.

Aeroelastic Effects

The test data presented include all aeroelastic effects that may be present. During the programing of the tests, it was assumed that these aeroelastic effects on C_{l_p} would be small in that the wings were made as stiff as practicable commensurate with efficient model-fabrication practices and static-stability requirements. When 60° sweptback wings like those in figures 3(b) and 3(c) gave much less damping than expected, it was strongly suspected that aeroelasticity was the cause. Inasmuch as the wings could not be made appreciably stiffer over the types of construction shown in figure 2 and wings of much reduced stiffness failed, no quantitative effects of aeroelasticity could be determined using the torque-nozzle technique alone. However, the actual stiffness characteristics of the test wings (listed in table I) give an insight into the aeroelastic effects. Shown in figure 10 are typical values of θ/m as a function of sweep for wings of no taper, moderate taper ($\lambda \approx 0.6$), and high taper ($\lambda \approx 0.3$) for the three methods of construction used. These measured stiffnesses illustrate that when a wing is swept more than 45° the stiffness is severely decreased even when the wing is of solid duralumin; hence, the effects of aeroelasticity on 60° swept wings as previously suspected were verified. Moreover, the value of $\frac{\theta}{m} = 10.450 \times 10^{-4}$

for the wing with $A = 6$ and $\Lambda = 45^\circ$ (plate-only construction of fig. 4(c)) accounts for the fact that the value of C_{l_p} obtained was lower than expected

By examination of the values of $\frac{(\theta/m)_{sd}}{\theta/m}$, the figure of merit, listed in table I, it may be seen that most of the wings were as stiff as solid duralumin and those that were not measured were of the inlay-plus-plate construction which usually gave θ/m values approaching those for solid duralumin. Consequently, the damping-in-roll results from the torque-nozzle technique are less affected by aeroelasticity (with exception of the two wings with plates only) than full-scale-aircraft wings which are not likely to be as stiff as solid duralumin wings. In any event, the aeroelastic effect of the decrease in stiffness (fig. 10) at sweep angles greater than 45°, as shown by these rocket-model tests, will be manifested to an equal or greater extent in the damping in roll of full-scale-aircraft wings.

Comparisons With Theory

In order to show the basic data in relation to available theory, a comparison of the experimental values of C_{l_p} with the theoretical values of C_{l_p} is shown in figure 11. The theory for the unswept wings is for two semispan wings from reference 11, the swept-wing theory is for two semispan wings from references 12 and 13, and the delta-wing theory is for three semispan wings from reference 14. This figure shows the values of C_{l_p} from experiment to roughly parallel the theory but is consistently lower than the predicted theoretical value. Most of this difference may be chargeable to the differences between linear theory and actual practice such as finite wing thickness, body effects, and so forth, and some of the difference is due to the aeroelastic effect on C_{l_p}. This aeroelastic effect can readily be seen in figure 11(b) in which the swept wing with the plate-only construction had much less C_{l_p} than either the other experiments or theory. Inasmuch as little aeroelastic effects are believed present in the delta-wing results, it is interesting to note in figure 11(c) that theory predicts the C_{l_p} better as the delta wings are given successively greater sweepback or lower aspect ratio.

CONCLUDING REMARKS

This collection of data indicates that the zero-lift damping in roll is well defined at transonic and low supersonic speeds for wing-body combinations having wings of aspect ratio less than 6 and ratios of body diameter to wing span near 0.2. Additional data will be needed for the higher Mach numbers, effects of external stores, effects of angle of attack, and for specific configurations.

The trends of the effects of the various geometric parameters are about as predicted by theory, when available, even though the level of damping is consistently lower than that obtained by theory and the existence of aeroelasticity must be considered in determining the damping in roll. This collection of damping-in-roll data from the rocket-model torque-nozzle technique lead to the following conclusions:

1. The plan-form effects are as follows:
   (a) Increased sweepback decreased damping in roll.
   (b) Decreased aspect ratio slightly decreased damping in roll.
   (c) Increased taper did not decrease damping in roll until tapered to a point.
   (d) Delta wings had lower values of damping in roll than other plan forms of comparable sweep or aspect ratio.

2. The airfoil-section effects are as follows:
   (a) Increased thickness ratio decreased damping in roll.
   (b) Section shape of unswept wings had a significant effect on the smoothness of the variation and the magnitude of the damping in roll with Mach number.

3. Increasing the number of semispan wings from three to four decreased damping in roll for unswept wings but had only a small effect for delta wings.

Langley Aeronautical Laboratory,
National Advisory Committee for Aeronautics,
Langley Field, Va., May 20, 1953.

REFERENCES

1. Edmondson, James L., and Sanders, E. Claude, Jr.: A Free-Flight Technique for Measuring Damping in Roll by Use of Rocket-Powered Models and Some Initial Results for Rectangular Wings. NACA RM L9I01, 1949.

2. Dietz, Albert E., and Edmondson, James L.: The Damping in Roll of Rocket-Powered Test Vehicles Having Rectangular Wings With NACA 65-006 and Symmetrical Double-Wedge Airfoil Sections of Aspect Ratio 4.5. NACA RM L50B10, 1950.

3. Edmondson, James L.: Damping in Roll of Rectangular Wings of Several Aspect Ratios and NACA 65A-Series Airfoil Sections of Several Thickness Ratios at Transonic and Supersonic Speeds As Determined With Rocket-Powered Models. NACA RM L50E26, 1950.

4. Bland, William M., Jr., and Dietz, Albert E.: Some Effects of Fuselage Interference, Wing Interference, and Sweepback on the Damping in Roll of Untapered Wings As Determined by Techniques Employing Rocket-Propelled Vehicles. NACA RM L51D25, 1951.

5. Sanders, E. Claude, Jr., and Edmondson, James L.: Damping in Roll of Rocket-Powered Test Vehicles Having Swept, Tapered Wings of Low Aspect Ratio. NACA RM L51G06, 1951.

6. Sanders, E. Claude, Jr.: Damping in Roll of Straight and 45° Swept Wings of Various Taper Ratios Determined at High Subsonic, Transonic, and Supersonic Speeds With Rocket-Powered Models. NACA RM L51H14, 1951.

7. Sanders, E. Claude, Jr.: Damping in Roll of Models With 45°, 60°, and 70° Delta Wings Determined at High Subsonic, Transonic, and Supersonic Speeds With Rocket-Powered Models. NACA RM L52D22a, 1952.

8. Strass, H. Kurt, Fields, E. M., and Purser, Paul E.: Experimental Determination of Effect of Structural Rigidity on Rolling Effectiveness of Some Straight and Swept Wings at Mach Numbers From 0.7 to 1.7. NACA RM L50G14b, 1950.

9. Stone, David G.: Wing-Dropping Characteristics of Some Straight and Swept Wings at Transonic Speeds As Determined With Rocket-Powered Models. NACA RM L50C01, 1950.

10. Purser, Paul E.: Notes on Low-Lift Buffeting and Wing Dropping at Mach Numbers Near 1. NACA RM L51A30, 1951.

11. Harmon, Sidney M.: Stability Derivatives at Supersonic Speeds of Thin Rectangular Wings With Diagonals Ahead of Tip Mach Lines. NACA Rep. 925, 1949. (Supersedes NACA TN 1706.)

12. Polhamus, Edward C.: A Simple Method of Estimating the Subsonic Lift and Damping in Roll of Sweptback Wings. NACA TN 1862, 1949.

13. Malvestuto, Frank S., Jr., Margolis, Kenneth, and Ribner, Herbert S.: Theoretical Lift and Damping in Roll at Supersonic Speeds of Thin Sweptback Tapered Wings With Streamwise Tips, Subsonic Leading Edges, and Supersonic Trailing Edges. NACA Rep. 970, 1950. (Supersedes NACA TN 1860.)

14. Ribner, Herbert S.: Damping in Roll of Cruciform and Some Related Delta Wings at Supersonic Speeds. NACA TN 2285, 1951.

TABLE I.- DATA FOR UNSWEPT, SWEPT, AND DELTA WINGS

	Λ, deg	A	λ	Airfoil section parallel to center line	D/b	Type construction, $\theta/m \times 10^4$, radians/ft-lb			$(\theta/m)_{ad}$ / θ/m	C_{l_p}			Figure number	Reference number
						Plate	Inlays + plate	Solid duralumin		M = 0.8	M = 1.0	M = 1.2		
Unswept wings	0	3.7	1.0	NACA 65A006	0.191		0.922		1.1	------	-0.378	-0.410	3(a),4(b),5(a),6(a)	1,6
	0	3.7	1.0	NACA 65A009	.191		.600		.5	------	-.354	-.367	4(a),6(a),9(a)	1,4
	0	2.5	1.0	NACA 65A009	.232		(a)		---	------	-.248	-.268	4(a)	3
	0	3.0	1.0	NACA 65A009	.212		(a)		---	------	-.300	-.325	4(a)	3
	0	4.5	1.0	NACA 65A009	.173		(a)		---	------	-.414	-.429	4(a),6(b)	3
	0	3.7	1.0	NACA 65_1A012	.191		(a)		---	-0.282	-.346	-.348	6(a)	3
	0	4.5	1.0	NACA 65-006	.181			1.533	1.0	-.350	-.416	-.407	4(b),6(b),7(a)	2
	0	4.5	1.0	Double wedge, $\frac{t}{c} = 0.06$	.181			2.156	1.0	------	-.417	-.511	7(a)	2
	0	3.7	.5	NACA 65A006	.191			.834	1.0	-.300	-.366	-.388	3(b),5(a)	6
	0	3.7	.3	NACA 65A006	.191			.684	1.0	------	-.354	-.379	3(c),5(a)	6
	0	3.7	0	NACA 65A006	.191		.615		1.1	-.242	-.300	-.312	5(a)	6
Swept wings	35	3.5	0.56	NACA 63-010	0.191		0.554		0.5	-0.218	-0.239	-0.240	4(c),6(c)	5
	35	3.5	.56	NACA 63-010 root / NACA 63-012 tip	.191		.512		.5	------	-.215	-.227	6(c)	5
	35	4.0	.6	NACA 65A006	.139		1.135		.8	-.268	-.261	-.250	3(b)	5
	40	4.0	.5	Circular arc, $\frac{t}{c} = 0.07$	.179		1.200		1.0	-.243	-.237	------	7(b)	5
	40	4.0	.5	Modified circular arc, $\frac{t}{c} = 0.07$	.179		1.146		1.0	-.258	-.270	-.289	7(b)	5
	45	4.0	.6	NACA 65A006	.139		1.126		1.0	-.253	-.250	------	3(b)	5
	45	3.7	.3	NACA 65A006	.191			1.089	1.0	------	-.271	-.268	3(c),5(b)	6
	45	3.7	.5	NACA 65A006	.191			1.312	1.0	-.270	-.274	-.280	5(b)	6
	45	3.7	1.0	NACA 65A006	.191		1.334		1.2	------	-.300	-.292	3(a),5(b)	6
	45	3.7	0	NACA 65A006	.191		1.674		1.0	------	-.212	-.210	5(b),8(a)	6
	45	6.0	.8	NACA 65A009	.150	10.450			.2	-.245	-.210	-.166	4(c)	5
	60	4.0	.6	NACA 65A006	.184	6.460			.8	-.120	-.104	-.090	3(b)	5
	61	3.5	.25	NACA 65A005	.186			2.739	1.0	------	-.157	-.150	3(c)	5
Delta wings (A_{LE})	45	4.0	0	NACA 65A006	0.170		(a)		---	------	-0.250	-0.238	8(a),9(b)	7
	60	2.31	0	NACA 65A006	.212		(a)		---	------	-.160	-.158	8(a),8(b),9(c)	7
	60	2.31	0	Hexagonal $\frac{t}{c} = 0.09$, tip; $\frac{t}{c} = 0.03$, root	.226		(a)		---	-0.140	-.152	-.168	8(b)	7
	70	1.45	0	NACA 65A006	.252		(a)		---	-.128	-.122	-.117	8(a),9(d)	7

[a]Not measured.

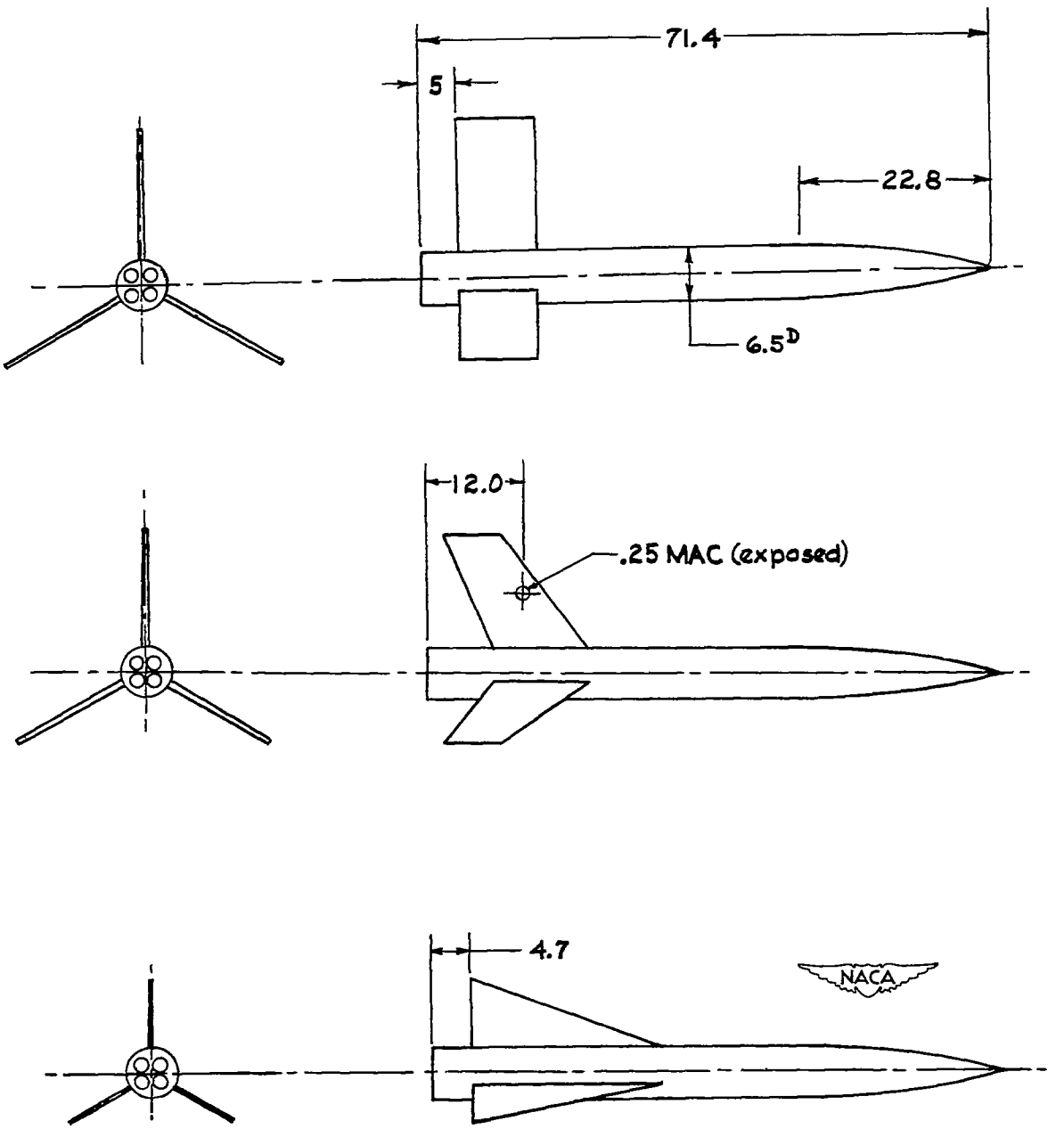

Figure 1.- Typical rocket-model shape for measuring damping in roll by the torque-nozzle technique. All dimensions are in inches.

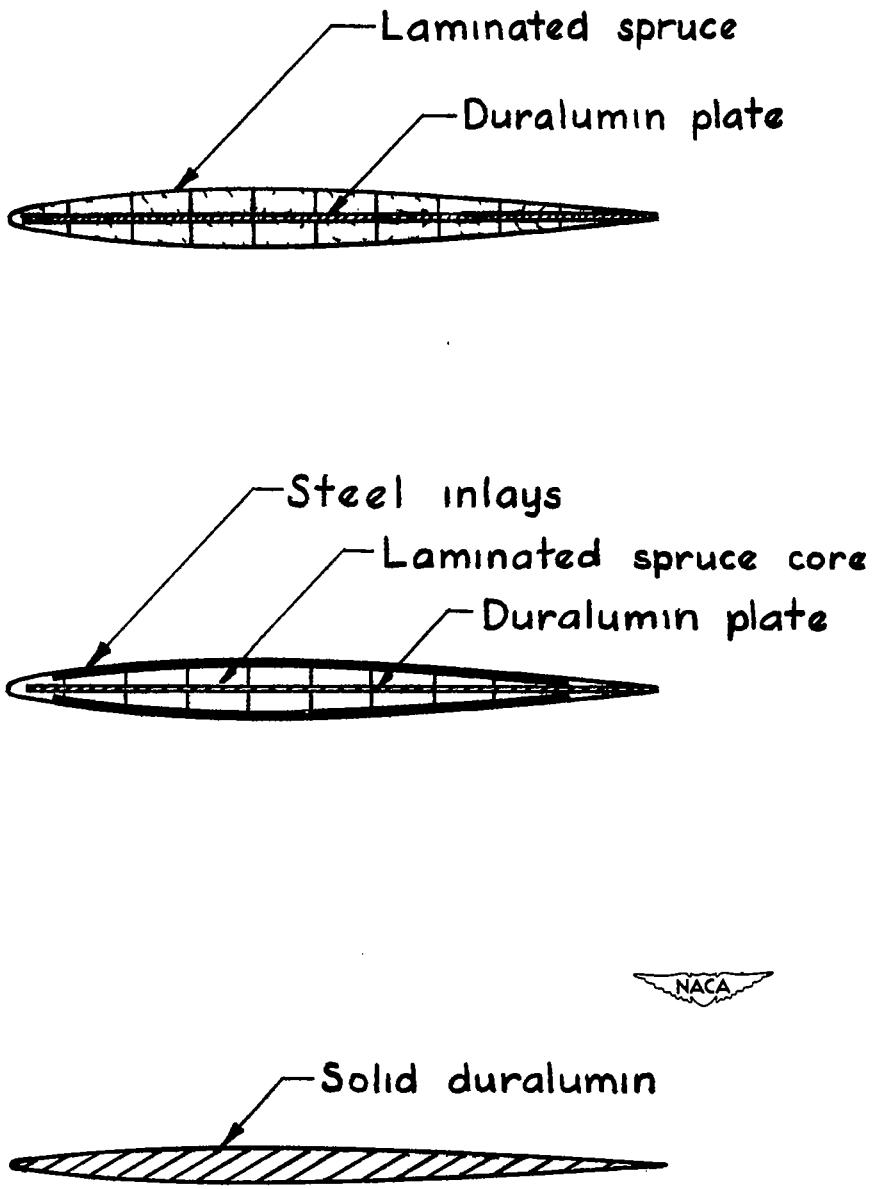

Figure 2.- Three different types of wing construction used on the damping-in-roll rocket models.

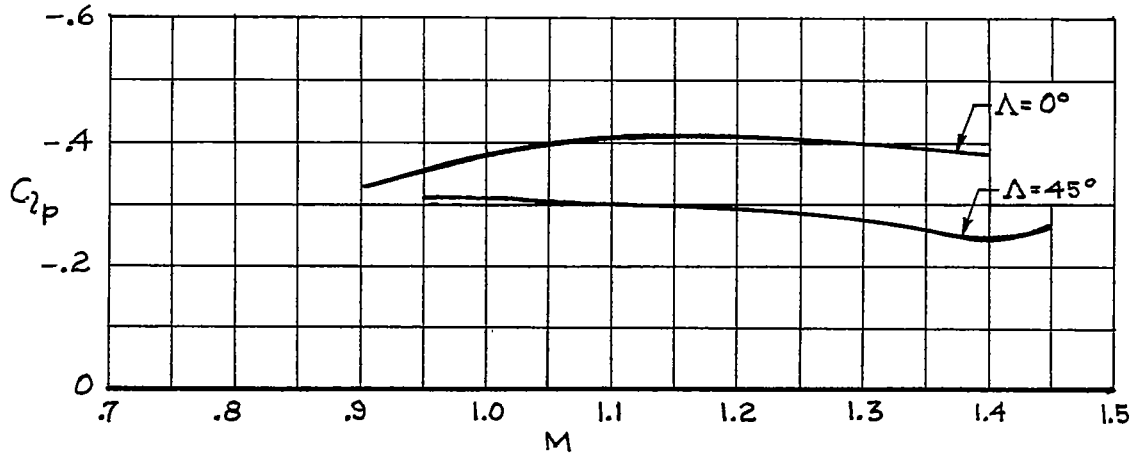

(a) Untapered wings. A = 3.7; NACA 65A006 airfoil sections.

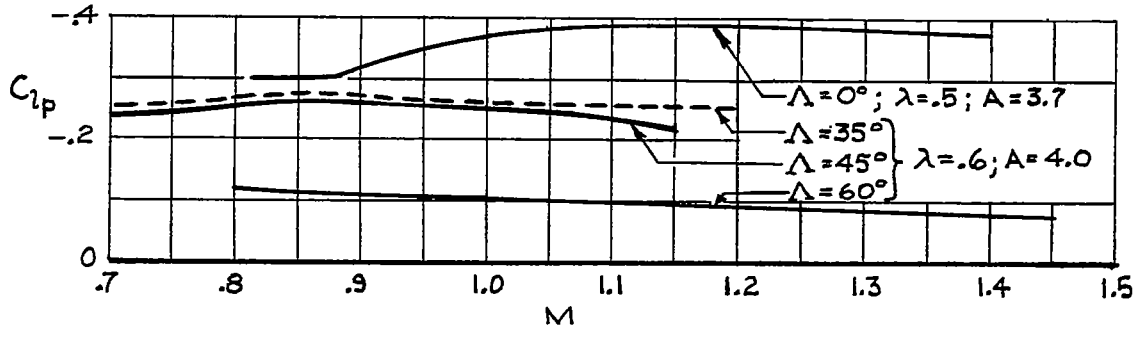

(b) Moderately tapered wings. NACA 65A006 airfoil sections.

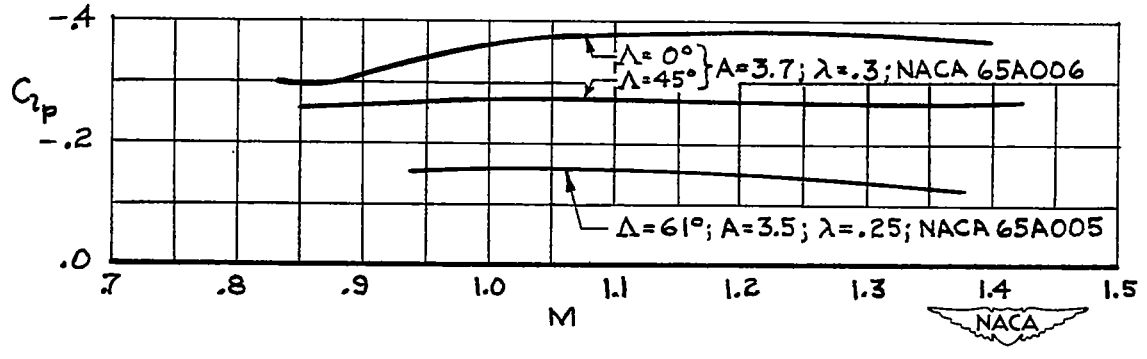

(c) Highly tapered wings.

Figure 3.- Effect of sweepback of quarter-chord line on damping in roll.

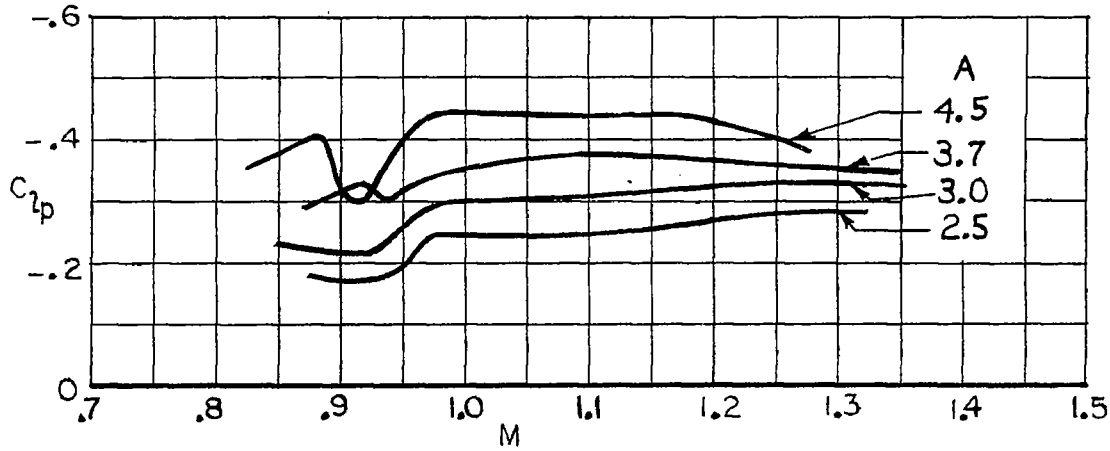

(a) Unswept wings. λ = 1.0; NACA 65A009 airfoil sections.

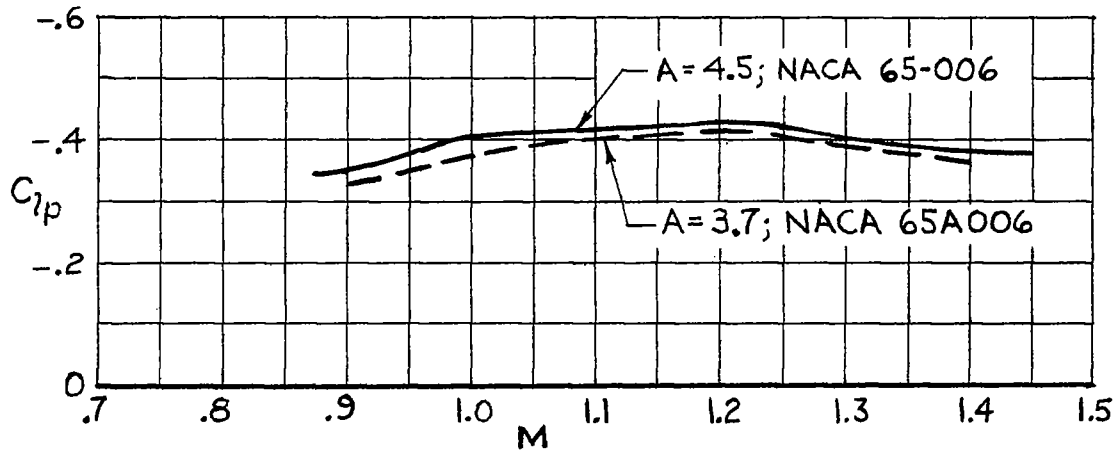

(b) Unswept wings. λ = 1.0; 6-percent-thick sections.

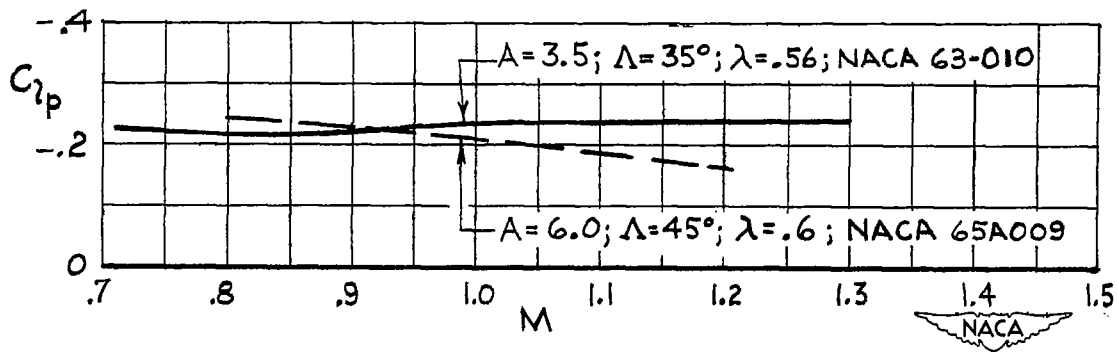

(c) Swept tapered wings.

Figure 4.- Effect of aspect ratio on damping in roll.

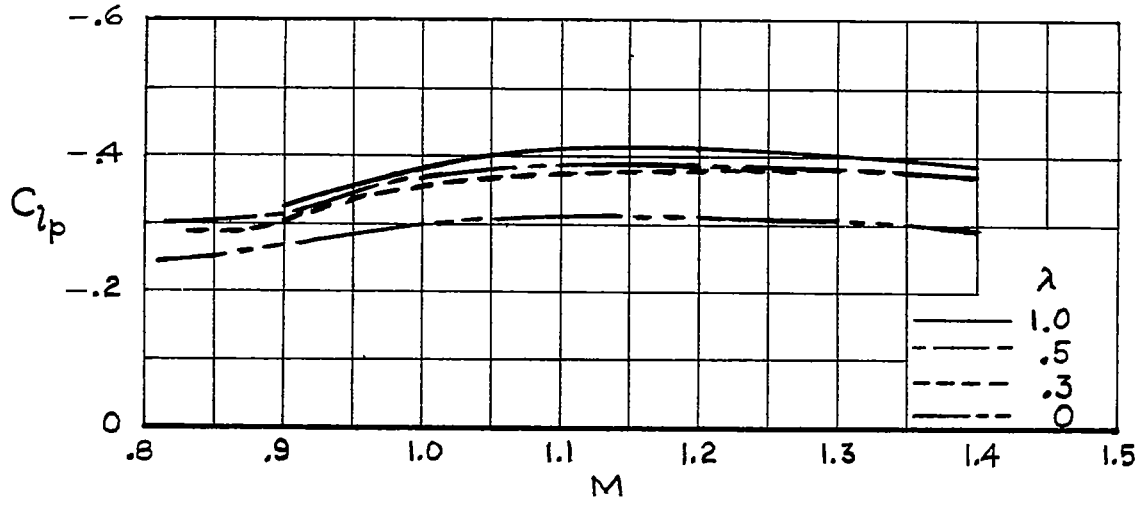

(a) Unswept wings. A = 3.7; NACA 65A006 airfoil sections.

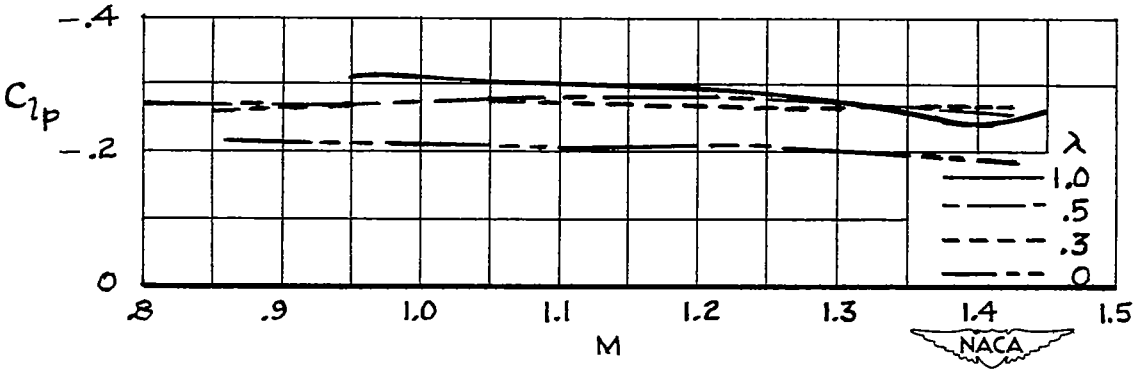

(b) 45° sweptback wings. A = 3.7; NACA 65A006 airfoil sections.

Figure 5.- Effect of taper ratio on damping in roll.

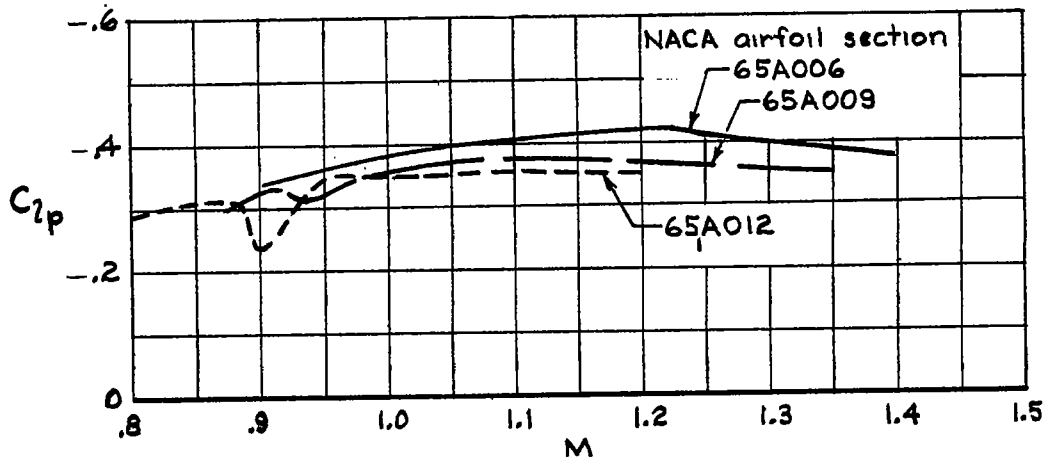

(a) Unswept wings. A = 3.7; λ = 1.0.

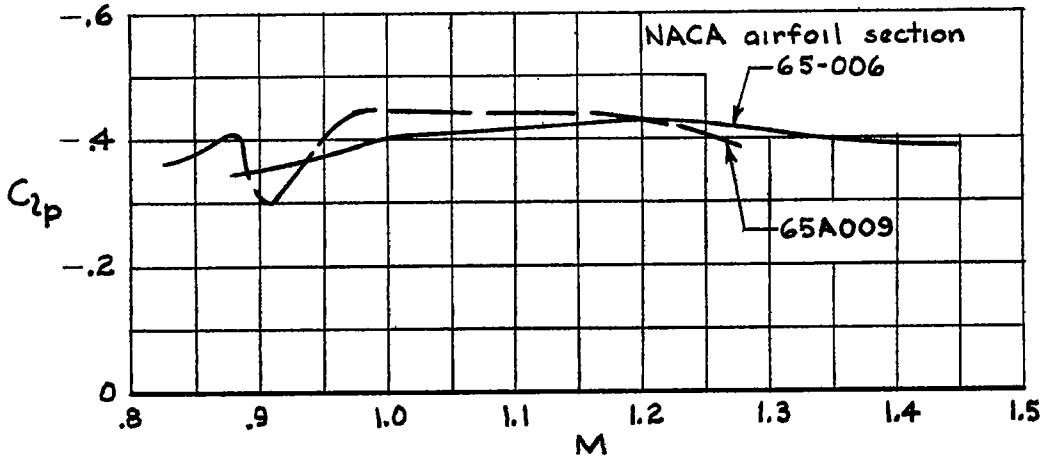

(b) Unswept wings. A = 4.5; λ = 1.0.

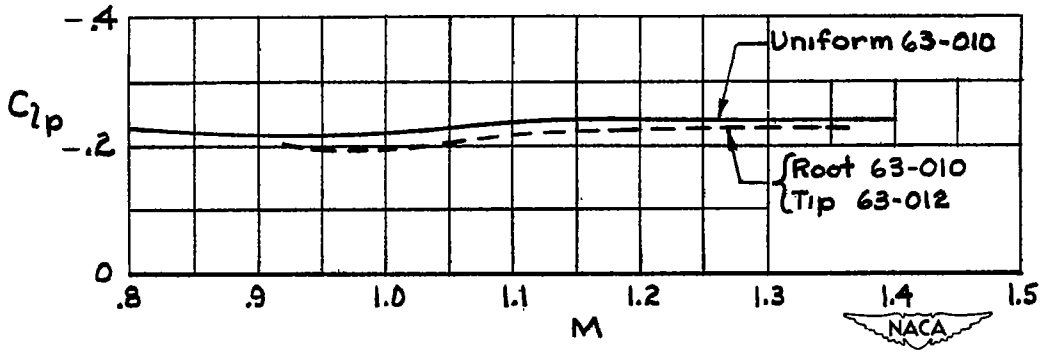

(c) 35° sweptback wings. A = 3.5; λ = 0.56;
NACA 63-series airfoil sections.

Figure 6.- Effect of airfoil-section thickness ratio on damping in roll.

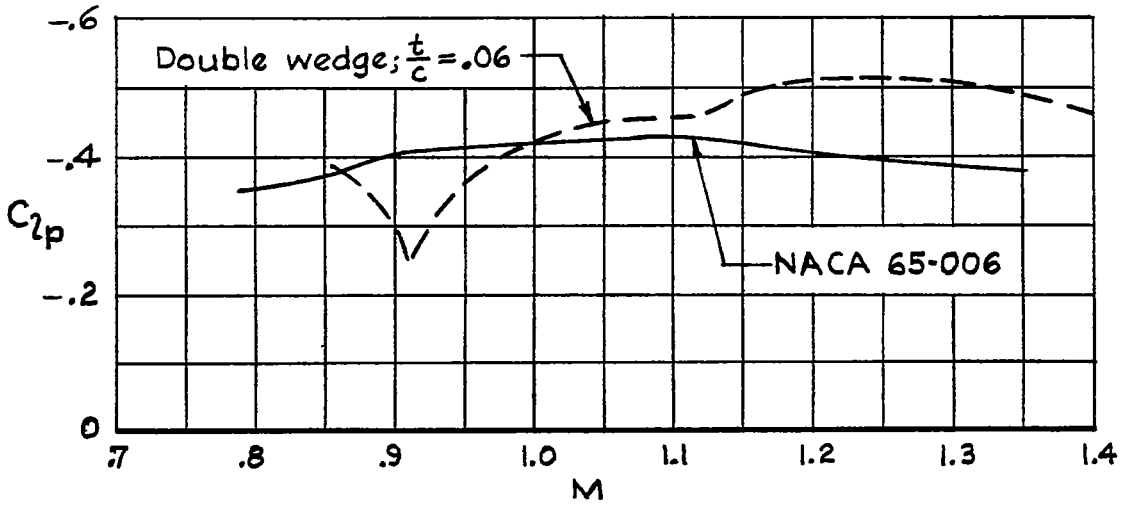

(a) Unswept wings. A = 4.5; λ = 1.0.

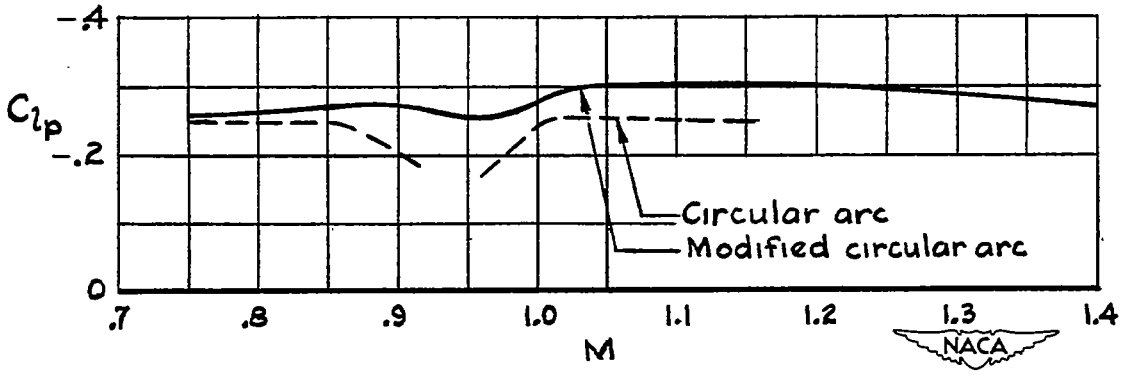

(b) 40° sweptback wings. A = 4.0; λ = 0.5; $\frac{t}{c}$ = 0.07.

Figure 7.- Effect of airfoil-section shape on damping in roll.

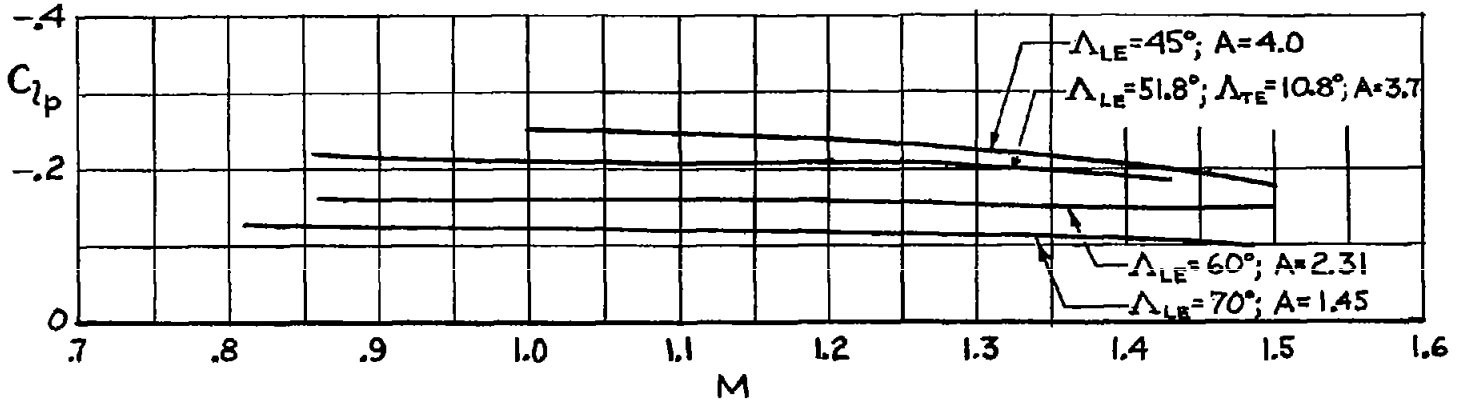

(a) Delta wings. NACA 65A006 airfoil sections.

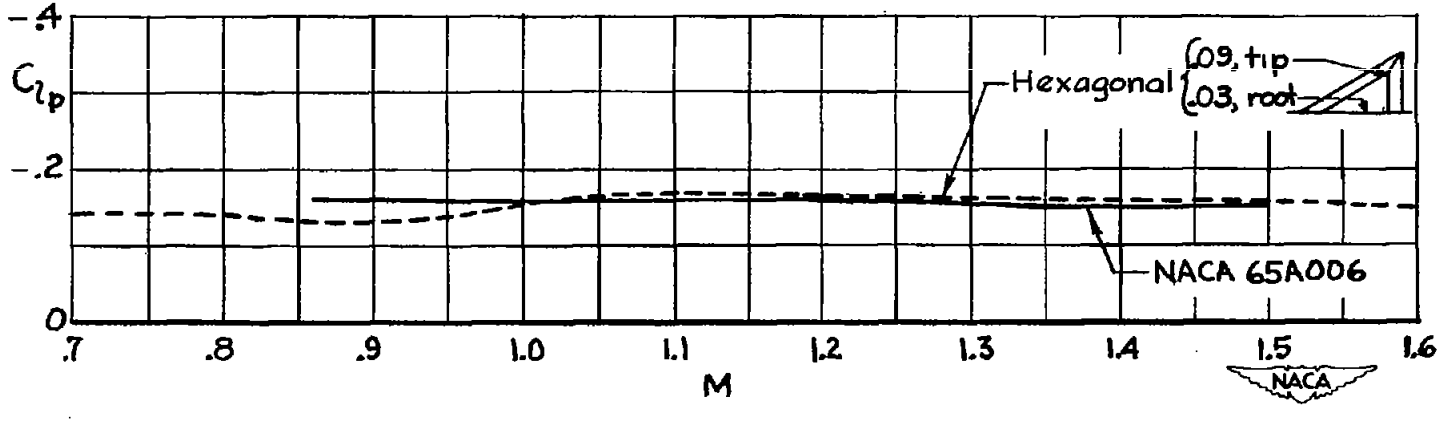

(b) Delta wings. Λ_{LE} = 60°; A = 2.31.

Figure 8.- Damping in roll of delta wings with various leading-edge sweep angles.

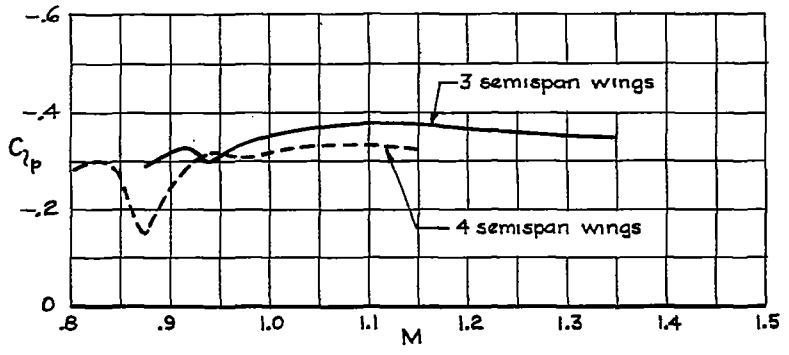

(a) Unswept wings. A = 3.7; λ = 1.0; NACA 65A009 airfoil sections.

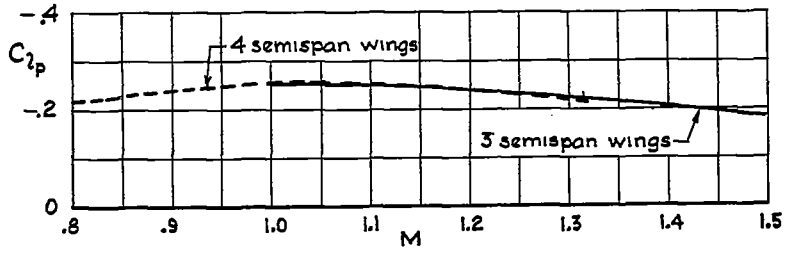

(b) 45° delta wings. A = 4.0; NACA 65A006 airfoil sections.

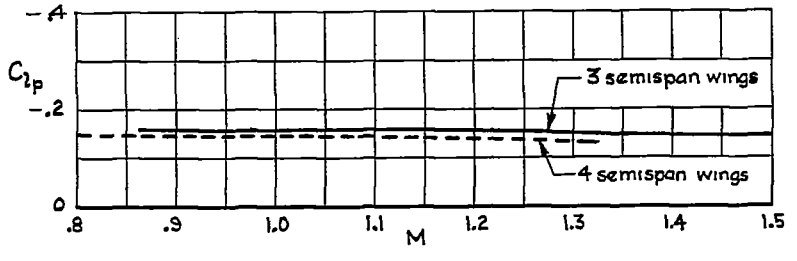

(c) 60° delta wings. A = 2.31; NACA 65A006 airfoil sections.

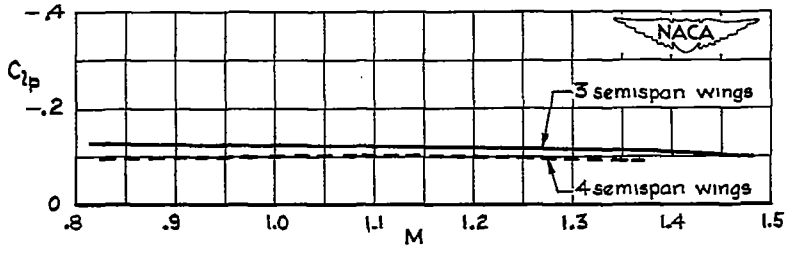

(d) 70° delta wings. A = 1.45; NACA 65A006 airfoil sections.

Figure 9.- Effect of increasing the number of semispan wings from three to four on the damping in roll.

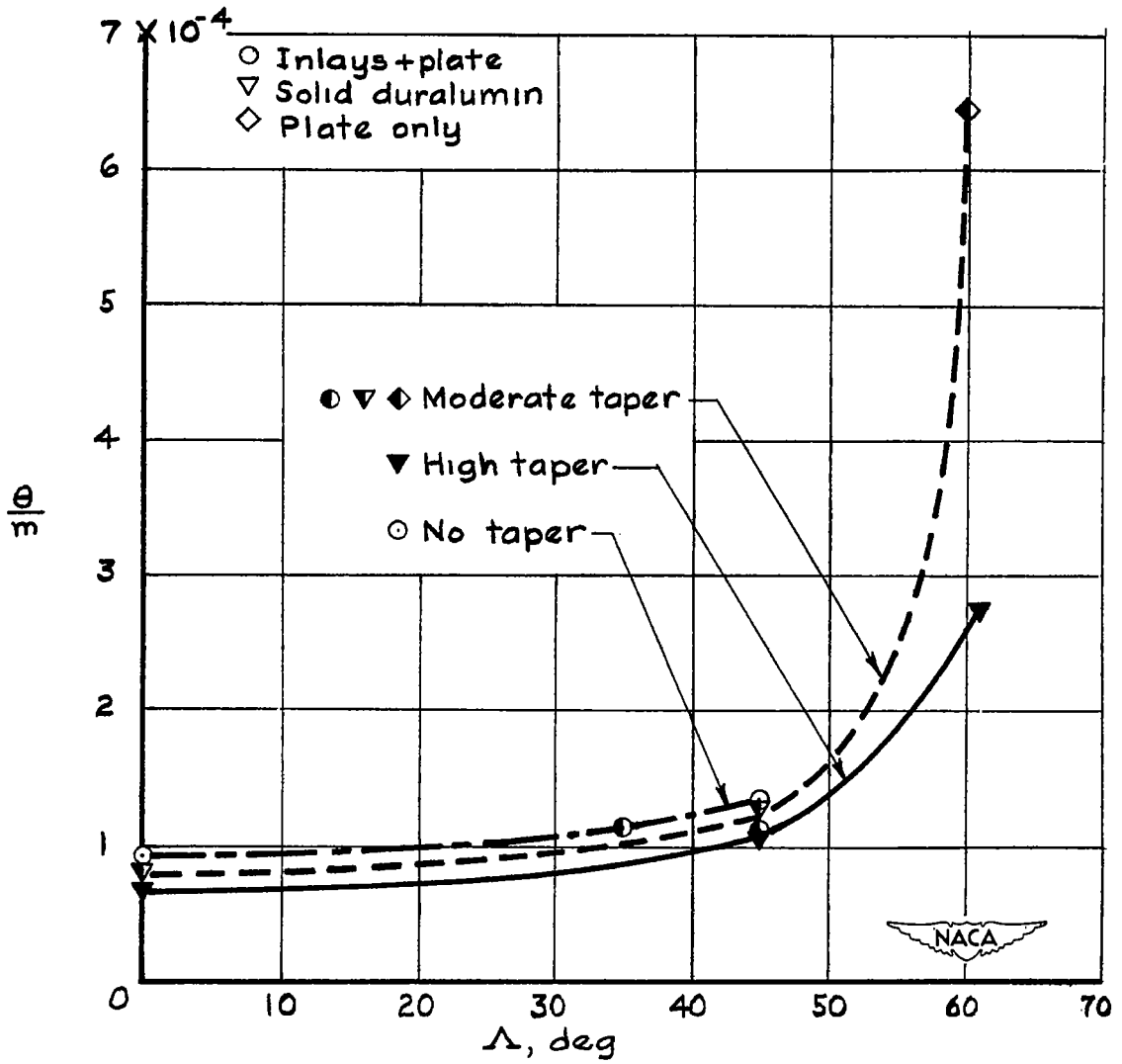

Figure 10.- Typical measured elastic characteristics of wings tested having NACA 65-series airfoil sections.

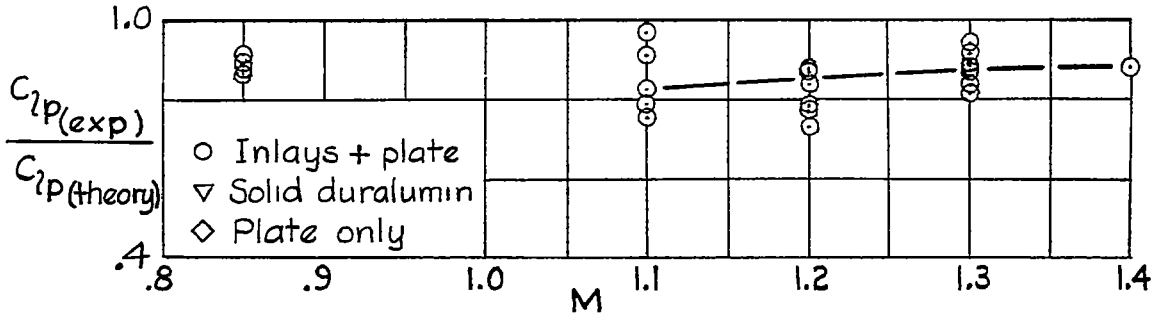

(a) Unswept wings. Theory from reference 11.

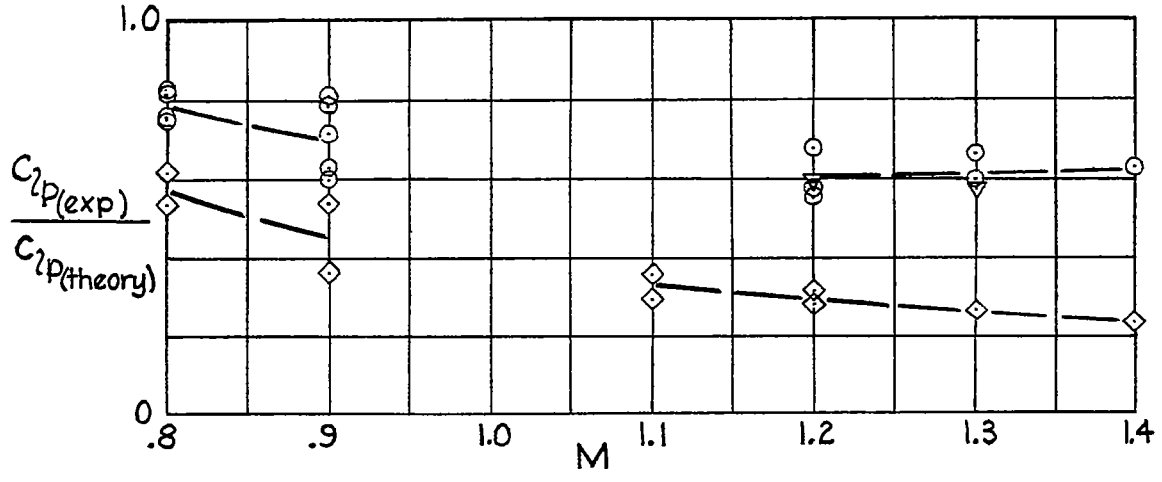

(b) Sweptback wings. Theory from references 12 and 13.

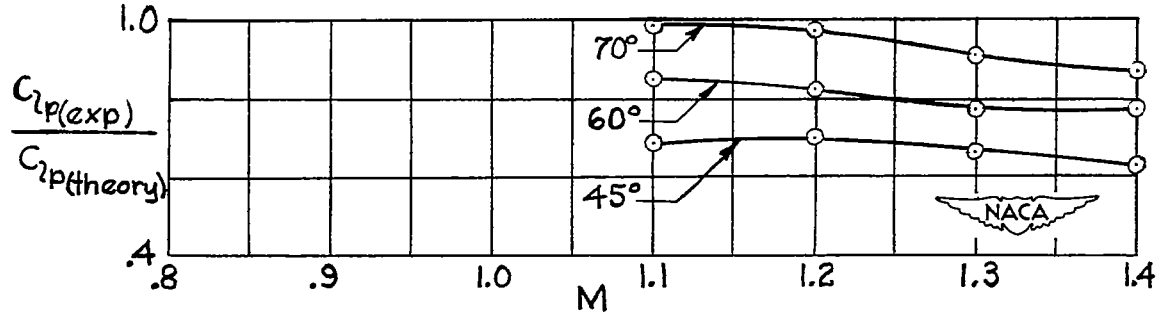

(c) Delta wings. Theory from reference 14.

Figure 11.- Ratio of the C_{l_p} from experiment to the C_{l_p} from theory with different types of wing construction.

NACA - Langley Field, Va.